Clin Pharmacol Ther. Author manuscript; available in PMC 2013 June 18.

Published in final edited form as:
Clin Pharmacol Ther. 2012 February ; 91(2): 227–233. doi:10.1038/clpt.2011.217.

P-glycoprotein mediated interaction between (*R*)-[^{11}C]verapamil and tariquidar at the human blood-brain barrier studied with positron emission tomography, a comparison with rat data

Martin Bauer[1], **Markus Zeitlinger**[1,*], **Rudolf Karch**[2], **Peter Matzneller**[1], **Johann Stanek**[1], **Walter Jäger**[3], **Michaela Böhmdorfer**[3], **Wolfgang Wadsak**[4], **Markus Mitterhauser**[4], **Jens P. Bankstahl**[5], **Wolfgang Löscher**[5], **Matthias Koepp**[6], **Markus Müller**[1], and **Oliver Langer**[1,7]

[1]Department of Clinical Pharmacology, Medical University of Vienna, Austria

[2]Center for Medical Statistics, Informatics and Intelligent Systems, Medical University of Vienna, Austria

[3]Department of Clinical Pharmacy and Diagnostics, University of Vienna, Austria

[4]Department of Nuclear Medicine, Medical University of Vienna, Austria

[5]Department of Pharmacology, Toxicology & Pharmacy, University of Veterinary Medicine Hannover, Germany

[6]Department of Clinical and Experimental Epilepsy, Institute of Neurology, University College London, UK

[7]Health and Environment Department, Molecular Medicine, AIT Austrian Institute of Technology GmbH, Seibersdorf, Austria

Abstract

Using positron emission tomography (PET) imaging we assessed *in vivo* the interaction between a microdose of (*R*)-[^{11}C]verapamil, a P-glycoprotein (Pgp) substrate, and escalating doses of the Pgp inhibitor tariquidar (3, 4, 6 and 8 mg/kg) at the blood-brain barrier (BBB) of healthy human subjects. We compared the dose-response relationship of tariquidar in humans with data obtained in rats using similar methodology. Tariquidar was equipotent in humans and rats to increase (*R*)-[^{11}C]verapamil brain uptake, expressed as whole brain volume of distribution (V_T), with very similar half-maximum effect concentrations. Both in humans and rats, brain V_Ts approached plateau levels at tariquidar plasma concentrations >1,000 ng/mL. However, Pgp inhibition in humans only led to 2.7-fold increase in brain V_T relative to baseline scans without tariquidar compared to 11.0-fold in rats. The results of this translational study add to the accumulating evidence of marked species-dependent differences in Pgp expression and functionality at the BBB.

*Corresponding author: Markus Zeitlinger, Department of Clinical Pharmacology, Division of Clinical Pharmacokinetics and Imaging, Medical University of Vienna, Währinger-Gürtel 18-20, 1090 Vienna, Austria; markus.zeitlinger@meduniwien.ac.at; Telephone: +43 1 40400 2981, Fax: +43 1 40400 2998..

Supplementary material
Supplementary information is available at http://www.nature.com/cpt.

Conflict of interest
The authors declare that they have no conflict of interest.

Europe PMC Funders Author Manuscripts

Keywords

P-glycoprotein; blood-brain barrier; drug-drug interaction; positron emission tomography; (*R*)-[^{11}C]verapamil; tariquidar; human; rat

Introduction

The adenosine triphosphate (ATP) binding cassette (ABC) transporter P-glycoprotein (Pgp, ABCB1) is expressed in the luminal membrane of the small intestine and blood-brain barrier (BBB), and in the apical membranes of excretory cells such as hepatocytes and kidney proximal tubule epithelia (1). Pgp actively transports a wide range of structurally diverse, mostly lipophilic, compounds against concentration gradients. Accordingly, there is an increasing demand by regulatory authorities to assess the interaction profile of new drug candidates with Pgp and other ABC transporters. Transport of drug candidates by Pgp is mostly considered a highly undesired property as it may have a significant impact on drug absorption, distribution and excretion or lead to drug-drug interactions (DDIs) with co-administered Pgp modulating drugs. In addition, polymorphisms in the *ABCB1* gene may lead to variable pharmacokinetics of Pgp substrate drugs (2). Examples of clinically relevant Pgp-mediated DDIs include interaction of digoxin with quinidine, ritonavir, dronedarone or ranolazine pharmacokinetics (1).

At the BBB, Pgp limits brain entry of several known drugs targeting the central nervous system, such as different anticancer, antiviral and antiepileptic drugs, thereby preventing therapeutically effective drug levels in the brain (3). Many drugs fail in late stage of clinical development because of reduced efficacy, or increased toxicity because they reach toxic concentration levels in areas affected differently by Pgp extrusion than the target area. Consequently, it is important to accurately predict the impact of Pgp efflux on drug brain distribution in humans during drug development. Several different approaches are available, including *in silico, in vitro* and *in vivo* methods (4). A commonly used *in vivo* approach compares brain distribution of candidate drugs in wild-type *versus* Pgp knockout (*Mdr1a/b*$^{(-/-)}$) mice. However, this approach overestimates the influence of Pgp on drug brain distribution in humans as it represents a “worst case” scenario, with no Pgp activity at the BBB. Furthermore, there is evidence for differences between rodents and humans in the expression levels (5) as well as in substrate and inhibitor specificity of Pgp and other ABC transporters, which often show overlapping affinity for Pgp substrates (6-10). In general, a better methodology is urgently needed to better understand species-dependent differences in Pgp. This would greatly improve our ability to predict human data either by direct measurement or by extrapolation from rodent data.

A highly powerful translational research tool to assess brain distribution of radiolabeled drugs is the non-invasive nuclear imaging method positron emission tomography (PET) (11). PET imaging with radiolabeled Pgp substrates, such as racemic [^{11}C]verapamil, (*R*)-[^{11}C]verapamil, [^{11}C]loperamide or [^{11}C]-*N*-desmethyl-loperamide, has been used to assess DDIs with Pgp modulators, such as cyclosporine A, valspodar and tariquidar, at the BBB, both in animals and humans (12-21). Results from these studies suggest that Pgp is less critical for drug distribution in the human than the rodent brain (22). However, whereas it was possible to employ different doses of Pgp modulators in animal studies (12,19) to provide dose-response relationships, this has not been done in human studies except for one radiotracer (20).

In the present study we assessed the effect of escalating doses of the potent third-generation Pgp inhibitor tariquidar (XR9576) (23) on brain uptake of a microdose of the radiolabeled

Europe PMC Funders Author Manuscripts

model Pgp substrate (*R*)-[^{11}C]verapamil (16,24-26) in healthy human subjects and compared the dose-response relationship of tariquidar with previously acquired rat data (19) providing us with the unique opportunity to directly compare the influence of Pgp on drug brain distribution in rodents and humans.

Results

Supplementary Table S1 online summarizes all adverse events which occurred during the study. Tariquidar was generally well tolerated. The most common side effects for which a relationship with the study drug could not be excluded were dysgeusia (6 out of 20 subjects) and vertigo (3 subjects). All adverse events were considered mild except for one case of moderate hypotension. In this subject the tariquidar infusion was stopped 20 min prematurely resulting in an administered tariquidar dose of 7.2 mg/kg. After discontinuing the infusion, the subject recovered quickly and the PET scan and other procedures were done as scheduled. Data from this subject were included in the 8 mg/kg dose group.

Administration of tariquidar at different doses did not affect the concentration of unmetabolized (*R*)-[^{11}C]verapamil in plasma (Figure 1). Pairwise comparison of the areas under the curve (AUC) from 0-40 min in Figure 1 of the 0 mg/kg dose group with the other dose groups gave *P* values >0.2 (Student's 2-sided t-test). Increasing doses of tariquidar resulted in a dose-dependent increase in brain concentration of (*R*)-[^{11}C]verapamil activity (Figure 2). In scans without tariquidar administration, brain activity uptake was low with the highest activity uptake observed in choroid plexus and venous sinus (Figure 2a), whereas under conditions of Pgp inhibition activity uptake was increased to similar levels throughout the brain (Figure 2c). Figure 3 shows mean time-activity curves (TACs) at baseline and after administration of different tariquidar doses. There was a dose-dependent increase in brain TACs following administration of the 2, 3, 4 and 6 mg/kg tariquidar doses. However, mean TACs of the 8 mg/kg dose group were lower than for the 6 mg/kg dose group, which is possibly due to lower tariquidar plasma levels at the end of the PET scan in 2 subjects of the 8 mg/kg dose group (Supplementary Table S2 online). PET data were analyzed quantitatively using 2-tissue-4-rate constant (2T4K) and 1-tissue-2-rate constant (1T2K) compartment models. Table 1 summarizes model outcome parameters for the different dose groups. Volume of distribution (V_T, 2T4K model), influx rate constant (K_1, 2T4K model) and K_1 (1T2K model) were the most sensitive parameters showing dose-dependent increases after administration of different tariquidar doses. Maximum increase relative to mean of baseline scans (i.e. without tariquidar administration) was 2.7-fold for V_T (2T4K model), 3.3-fold for K_1 (2T4K model) and 3.4-fold for K_1 (1T2K model). Supplementary Table S2 online summarizes tariquidar plasma concentration levels at the start and the end of the PET scan measured with liquid chromatography tandem mass spectrometry for the present study and the previously published pilot study (17). Tariquidar plasma concentrations were nearly constant through the duration of the PET scan in individual subjects, but concentration range varied among different subjects pertaining to the different dose groups (281-1,312 ng/mL). Sigmoidal Hill functions were fitted to absolute V_T increases (V_T- V_T baseline) and K_1 increases (K_1-K_1 baseline) at different tariquidar plasma concentrations and compared to data obtained in our previous rat study (19) (Figure 4). Outcome parameters of the sigmoidal fits are given in Table 2. Humans and rats showed similar half-maximum effect concentrations (EC_{50}) of tariquidar for all effect measures. For enhancement of V_T- V_T baseline, EC_{50} was 561±24 ng/mL in humans and 544±32 ng/mL in rats. However, maximum effect (E_{max}) values were 13-16-fold higher in rats than in humans. On the other hand, Hill coefficients (n) were lower in rats than in humans, pointing to different cooperativities in Pgp binding.

Discussion

Tariquidar has been developed as a potent third-generation Pgp inhibitor to overcome multidrug resistance in cancer (23). It has been tested in phase 1-3 clinical trials at doses up to 2 mg/kg. Its ability to inhibit Pgp *in vivo* has been assessed by studying rhodamine-123 efflux in CD56-positive lymphocytes as a surrogate marker, demonstrating that a single intravenous (i.v.) dose of 2 mg/kg tariquidar blocks Pgp in CD56-positive lymphocytes by 100% over 24 h (27). However, at the human BBB the 2 mg/kg dose was shown to exert only a small effect (+25%) on increasing brain penetration of the Pgp substrates (*R*)-[^{11}C]verapamil (17) and [^{11}C]-*N*-desmethyl-loperamide (20) suggesting that Pgp at the BBB is more resistant to inhibition than peripheral Pgp (28).

As we have previously shown in rats that performing (*R*)-[^{11}C]verapamil PET scans after half-maximum inhibition of Pgp by tariquidar is better suited to assess regional differences in cerebral Pgp function than baseline scans alone (29), we were interested in identifying the EC_{50} of tariquidar in humans in order to translate this concept to a clinical study protocol. Remarkably, our study showed that tariquidar was equipotent in rats and humans to inhibit Pgp at the BBB with very similar EC_{50} values (Table 2). This finding is noteworthy as for several other Pgp inhibitors species-dependent differences in inhibitory effects have been reported, both *in vitro* and *in vivo* (7-8). Moreover, we found that tariquidar was well tolerated at doses 4-times the clinically tried and lacked pharmacokinetic interactions with (*R*)-[^{11}C]verapamil (Figure 1), showing its superiority over cyclosporine A to study Pgp inhibition at the BBB. Furthermore, we have shown in previous studies that administration of tariquidar does not influence the degree of plasma protein binding of (*R*)-[^{11}C]verapamil (17,19). Apart from Pgp, tariquidar also inhibits breast cancer resistance protein (BCRP, ABCG2), another important ABC transporter expressed at the BBB (30). As (*R*)-[^{11}C]verapamil is not transported by BCRP at the BBB (31) we were able to selectively study cerebral Pgp inhibition using a combination of (*R*)-[^{11}C]verapamil and tariquidar.

In accordance with previous Pgp inhibition studies both in animals and humans (15-20,32), V_T and K_1, as calculated with a 2T4K compartment model, increased dose-dependently after tariquidar administration (Table 1, Figure 4). To minimize the influence on modeling outcome parameters of radiolabeled (*R*)-[^{11}C]verapamil metabolites, which are partly taken up into brain tissue independent of Pgp function and partly also display Pgp substrate properties (24,26), we only used first 10 min of PET data for analysis (32) (Table 1). K_1 values derived from the 1T2K model (0-10 min) were very similar to K_1 values from the 2T4K model (0-40 min) arguing against a significant effect of (*R*)-[^{11}C]verapamil metabolites on model-derived K_1 values (Table 1).

We observed a 2.5-fold whole brain V_T increase of (*R*)-[^{11}C]verapamil after 6 mg/kg tariquidar. Kreisl *et al.* (20) recently studied the effect of escalating tariquidar doses (up to 6 mg/kg) on brain uptake of [^{11}C]-*N*-desmethyl-loperamide in healthy human subjects. After the 6 mg/kg tariquidar dose, there was a 4-fold maximum increase of brain activity uptake (area under the cerebellar TAC from 10-30 min) compared to baseline scans without tariquidar. This difference is most likely due to the 2-fold lower baseline brain uptake of [^{11}C]-*N*-desmethyl-loperamide as compared to (*R*)-[^{11}C]verapamil suggesting that [^{11}C]-*N*-desmethyl-loperamide is more efficiently transported by Pgp than (*R*)-[^{11}C]verapamil. This is reasonable to assume as it is known that loperamide is a more avid Pgp substrate than verapamil (33). Kreisl and colleagues (20) did not use kinetic modeling in all subjects to provide quantitative measures of radiotracer brain distribution (V_T, K_1), nor did they report tariquidar plasma concentrations which makes it difficult to compare the (*R*)-[^{11}C]verapamil/tariquidar DDI described in our study with the [^{11}C]-*N*-desmethyl-loperamide/tariquidar DDI.

Nearly identical methodology as in a previous rat study (19) was used in the present clinical study which provided us with the unique opportunity to directly compare rat and human data. In rats, after bolus administration of 30 mg/kg tariquidar plasma concentrations up to 7,000 ng/mL were achieved at the time of the PET scan (19). In humans, the maximum administered tariquidar dose was 8 mg/kg, resulting in plasma concentrations up to 1,312 ng/mL at time of PET (Supplementary Table S2 online). In our study, tariquidar plasma levels did not increase linearly with administered dose, which is likely due to the fact that we had to prolong infusion with increasing tariquidar doses for safety reasons. Elimination of tariquidar from plasma was slow (terminal elimination half-life, 13-23 h (17)) resulting in stable plasma levels over the time course of the 1 h PET scan (Supplementary Table S2 online).

(*R*)-[^{11}C]verapamil baseline whole brain V_Ts were about 2-fold lower in humans than in rats (0.66±0.12 *versus* 1.27±0.15) which is unexpected given recent findings of about 3-fold higher Pgp expression levels at the rodent as compared to the human BBB (5). However, possible differences in Pgp activity or expression between rats and humans could have been blunted in the baseline scans by differences in radiotracer metabolism leading to a higher percentage of brain-penetrating radiolabeled metabolites in plasma of rats than in humans (19). Another factor which could explain the differences in (*R*)-[^{11}C]verapamil baseline brain V_Ts could be different unbound fractions of (*R*)-[^{11}C]verapamil in plasma of rats and humans. However, we have found previously that plasma unbound fractions of (*R*)-[^{11}C]verapamil were almost identical in rats and humans (rats: 0.069±0.02; humans: 0.070±0.02) (17).

Both in the rat and the human study, brain uptake of (*R*)-[^{11}C]verapamil approached plateau values after administration of increasing tariquidar doses, essentially at tariquidar plasma concentrations >1,000 ng/mL (Figure 4). Whereas it seems likely that complete inhibition of Pgp was reached at the rat BBB, as indicated by comparable activity concentration levels in rat brain after administration of tariquidar doses >6 mg/kg and in brains of *Mdr1a/b*$^{(-/-)}$ mice (31), it is not known whether the observed plateau indeed represented full Pgp inhibition in the human study.

We found a most striking difference in the concentration response-relationships of tariquidar with a 2.7-fold maximum increase in brain activity uptake compared to baseline in humans *versus* an 11.0-fold increase in rats (Figure 4). Similar differences between rats and humans have recently been pointed out for the [^{11}C]loperamide/cyclosporine A DDI at the BBB (34), although they were based on only one single dose level of cyclosporine A for the human study (21). [^{11}C]Verapamil brain uptake increased by 88% compared to baseline in humans after i.v. infusion of cyclosporine A (2.5 mg/kg/h) (13) whereas maximum increases of 1290% were found in a dose escalation study in rats (35). The observation that this pronounced difference in the magnitude of the Pgp inhibitory effect at the rat and human BBB is not specific for the (*R*)-[^{11}C]verapamil/tariquidar pair widely excludes the possibility that it might be only related to species-dependent differences in the pharmacokinetic and/or pharmacodynamic properties of the investigated compounds. A possible explanation for the observed differences in our study could be that, as opposed to rats, Pgp was only partially inhibited in humans, i.e. that radiotracer was still actively effluxed from brain under conditions of Pgp inhibition. In mice, the half-maximum effect dose (ED_{50}) of tariquidar to inhibit rhodamine-123 efflux in CD56-positive lymphocytes was shown to be 25-fold lower than the ED_{50} for enhancement of the brain-to-plasma ratio of loperamide (28). This was interpreted in a way that inhibitor first has to diffuse through the cellular membrane before it can reach the Pgp binding site facing the cytosol and that this diffusion barrier might be higher at the BBB than in peripheral cells (36). In analogy, it can be speculated that Pgp at the human BBB might be less accessible to inhibitor than Pgp

at the rat BBB leading to the observed differences in maximum inhibitory effects. Moreover, it has recently been shown that brain uptake of [^{11}C]-*N*-desmethyl-loperamide depends on cerebral blood flow under conditions of Pgp inhibition (15). Thus it is possible that differences in cerebral blood flow could have contributed to the observed differences in maximum (*R*)-[^{11}C]verapamil brain uptake as cerebral blood flow is higher in rats than in humans (37).

Taken together, our observation that drug brain distribution in humans was enhanced to a much lower degree under conditions of Pgp inhibition than in rodents adds to the accumulating evidence of marked species differences in Pgp expression and functionality at the BBB. Extending our translational DDI study to other sets of substrate/inhibitor pairs might help to provide a general understanding of the mechanisms underlying the observed species-dependent differences in drug brain distribution.

Methods

The study protocol was approved by the Ethics Committee of the Medical University of Vienna and was performed in accordance with the Declaration of Helsinki (1964) in the revised version of 2000 (Edinburgh), the Guidelines of the International Conference of Harmonization, the Good Clinical Practice Guidelines, and the Austrian drug law (Arzneimittelgesetz). All subjects were given a detailed description of the study, and their written consent was obtained before entry into the study.

The study was designed as a clinical study with escalating doses of 3, 4, 6 and 8 mg/kg body weight tariquidar. 20 healthy male subjects with a mean age of 31.1, standard deviation (SD) ±8.4 years and a mean body weight of 79.4±11.8 kg were included into the study and randomized to the 4 dose groups (5 subjects per dose group). Subjects were defined as healthy based on subjects' medical history, physical examination, routine blood and urine laboratory testing (including chemistries, complete blood count, liver and renal function tests), blood pressure, heart rate and electrocardiography (ECG). Subjects were free of any medication for at least 14 days before the study day. Data of this study were pooled with data from a previously published pilot study, in which five healthy subjects had undergone (*R*)-[^{11}C]verapamil PET scans before and after i.v. infusion of 2 mg/kg tariquidar (17).

Study medication

10-mL vials of tariquidar for i.v. infusion containing 7.5 mg/mL of tariquidar free base in 20% ethanol/80% propylene glycol were provided by AzaTrius Pharmaceuticals Pvt Ltd (London, UK). For the 3 mg/kg dose group, the volume (mL) of concentrate for injection was calculated as: body weight (kg) × 3/7.5. To the calculated volume of concentrate, aqueous dextrose solution (5%, w/v) was added to yield a final volume of 250 mL, which was administered i.v. *via* an antecubital vein over 30 min (17). As there is evidence that the co-solvent of tariquidar vials for i.v. infusion can cause hemolysis at concentrations >14.4% (38) a slightly modified administration schedule was adopted for the 4, 6 and 8 mg/kg dose groups (20). In brief, tariquidar was diluted in 5% dextrose solution to a fixed concentration of 0.6 mg/mL and infused i.v. at a rate of 375 mL/h until achieving the target dose.

Data acquisition

For safety reasons, the first two subjects of each dose group received the tariquidar infusion only, whereas the following three subjects underwent (*R*)-[^{11}C]verapamil PET imaging at 63±3 min after end of tariquidar infusion. (*R*)-[^{11}C]verapamil (379±9 MBq), containing <20 μg of unlabeled (*R*)-verapamil, was injected i.v. over 20 s and a dynamic PET scan consisting of 20 frames was recorded on an Advance PET scanner (GE Medical Systems,

Wukesha, WI, USA) for 60 min. During the PET scan arterial blood was manually sampled at approximately 5 s intervals for the first 2.5 min, then at time points of 3.5, 5, 10, 20, 30, 40, and 60 min after radiotracer injection. For analysis of radiolabeled metabolites of (*R*)-[^{11}C]verapamil a previously described combined solid-phase extraction/high-performance liquid chromatography (HPLC) assay was used (39). For construction of an arterial input function the arterial plasma activity data were corrected for polar [^{11}C]metabolites of (*R*)-[^{11}C]verapamil as described previously (17). As data were pooled with data from the pilot study, only the first 40 min of the PET and arterial input data were considered for kinetic modeling analysis (see below). In addition, AUCs from time 0 to 40 min were calculated for TACs of unmetabolized (*R*)-[^{11}C]verapamil in arterial plasma, normalized to the injected radiotracer amount per body weight and expressed as standardized uptake value (SUV), with a noncompartmental model using the Kinetica 2000 software package, version 3.0 (InnaPhase, Philadelphia, USA). At the start and the end of the PET scan venous blood samples (4 mL) were withdrawn in order to measure tariquidar concentration levels.

Determination of tariquidar plasma levels

The concentration of tariquidar in plasma was measured using a Dionex UltiMate 3000 system (Dionex Corp., Sunnyvale, CA, USA) connected with an API 4000 triple-quadrupole mass spectrometer (Applied Biosystems, Concord, Ontario, Canada). After addition of 200 μL of methanol to 100 μL of plasma, the samples were centrifuged (5,000 g for 5 min at 4°C) and 80 μL of the clear supernatant was injected onto the HPLC column. Separation of tariquidar was carried out at 35°C using a Hypersil BDS-C18 column (5 μm, 250 × 4.6 mm I.D., Thermo Fisher Scientific, Inc, Waltham, MA, USA), preceded by a Hypersil BDS-C18 pre-column (5 μm, 10 × 4.6 mm I.D.). The mobile phase consisted of a continuous linear gradient, mixed from 10 mM ammonium acetate/acetic acid buffer, pH 5.0 and methanol. Linear calibration curves were generated by spiking drug-free plasma with standard solutions of tariquidar (final concentrations ranging from 0.005 to 5 μg/mL). The lower limit of detection of tariquidar was 3 ng/mL and the lower limit of quantification 5 ng/mL.

Imaging data analysis

PET and high-resolution 3 tesla T1 weighed magnetic resonance imaging (MRI) data, which had been acquired within 3 weeks before or after the PET study day, were processed as described previously (17). Whole brain grey matter TACs were extracted by using the Hammersmith n30r83 three-dimensional maximum probability atlas of the human brain (40), as described previously (17).

Kinetic modeling

A standard 2T4K compartment model was fitted to the (*R*)-[^{11}C]verapamil TACs from time zero to 40 min in whole brain grey matter (17,41) to estimate V_T as well as the rate constants for transfer of activity between the plasma, the first and the second tissue compartments (K_1, k_2, k_3, k_4). For the 2T4K model, V_T is given as $(1+k_3/k_4) \times (K_1/k_2)$ and can be essentially considered as an estimate of the brain-to-plasma ratio of radioactivity at equilibrium. As a second analysis approach, which has been proposed recently by Muzi *et al.* (32), the influx rate constant of activity K_1 was estimated by using a 1T2K compartment model fitted to only the first 10 min of the PET data, a time span where the contribution of radiolabeled metabolites of (*R*)-[^{11}C]verapamil to the PET signal can be considered minimal.

Sigmoidal curves were fitted to different effect (*E*) measures (V_T-V_T baseline, 2T4K model; K_1-K_1 baseline, 2T4K model; K_1-K_1 baseline, 1T2K model) plotted against tariquidar

plasma concentrations using the following equation included in the OriginPro 7.5G software package (OriginLab Corporation, Northampton, MA, USA):

$$E = E_{\max} \frac{C^n}{(EC_{50}{}^n + C^n)},$$

where $E_{\max}$ is the maximum effect, C the tariquidar plasma concentration (ng/mL), EC_{50} the half-maximum effect concentration of tariquidar (ng/mL), and n the Hill coefficient. To enable better comparability with our rat data (19), where tariquidar plasma concentrations could only be measured at the end of the PET scan, we also used tariquidar plasma concentrations at the end of the PET scan for the human dataset.

Safety monitoring

Subjects were monitored for changes in ECG, blood pressure and heart rate before and at least 7 time points during and until 24 h after tariquidar infusion. Blood laboratory tests were repeated 24 h after end of tariquidar infusion and at final visit within one week thereafter. At every visit adverse events were recorded.

Supplementary Material

Refer to Web version on PubMed Central for supplementary material.

Acknowledgments

The research leading to these results has received funding from the European Community's Seventh Framework Program under grant agreement no. 201380 (Euripides) and from the Austrian Science Fund (FWF) project "Transmembrane Transporters in Health and Disease" (SFB F35). Edith Lackner, Maria Weber, Denis Todorut (all Department of Clinical Pharmacology) and Rainer Bartosch and Bettina Reiterits (Department of Nuclear Medicine) are acknowledged for excellent technical support and AzaTrius Pharmaceuticals Pvt Ltd (London, UK) for providing tariquidar vials for i.v. infusion. Claudia Kuntner (AIT Austrian Institute of Technology GmbH) is acknowledged for providing the (*R*)-[^{11}C]verapamil rat data.

References

1. Giacomini KM, et al. Membrane transporters in drug development. Nat. Rev. Drug Discov. 2010; 9:215–236. [PubMed: 20190787]
2. Chinn LW, Kroetz DL. ABCB1 pharmacogenetics: progress, pitfalls, and promise. Clin. Pharmacol. Ther. 2007; 81:265–269. [PubMed: 17259950]
3. Löscher W, Potschka H. Role of drug efflux transporters in the brain for drug disposition and treatment of brain diseases. Prog. Neurobiol. 2005; 76:22–76. [PubMed: 16011870]
4. Hammarlund-Udenaes M, Bredberg U, Friden M. Methodologies to assess brain drug delivery in lead optimization. Curr. Top. Med. Chem. 2009; 9:148–162. [PubMed: 19200002]
5. Uchida Y, et al. Quantitative targeted absolute proteomics of human blood-brain barrier transporters and receptors. J. Neurochem. 2011; 117:333–345. [PubMed: 21291474]
6. Luna-Tortos C, Fedrowitz M, Löscher W. Several major antiepileptic drugs are substrates for human P-glycoprotein. Neuropharmacology. 2008; 55:1364–1375. [PubMed: 18824002]
7. Cutler L, Howes C, Deeks NJ, Buck TL, Jeffrey P. Development of a P-glycoprotein knockout model in rodents to define species differences in its functional effect at the blood-brain barrier. J. Pharm. Sci. 2006; 95:1944–1953. [PubMed: 16850390]
8. Suzuyama N, et al. Species differences of inhibitory effects on P-glycoprotein-mediated drug transport. J. Pharm. Sci. 2007; 96:1609–1618. [PubMed: 17094122]

9. Takeuchi T, et al. Establishment and characterization of the transformants stably-expressing MDR1 derived from various animal species in LLC-PK1. Pharm. Res. 2006; 23:1460–1472. [PubMed: 16779700]
10. Katoh M, Suzuyama N, Takeuchi T, Yoshitomi S, Asahi S, Yokoi T. Kinetic analyses for species differences in P-glycoprotein-mediated drug transport. J. Pharm. Sci. 2006; 95:2673–2683. [PubMed: 16892207]
11. Wagner CC, Müller M, Lappin G, Langer O. Positron emission tomography for use in microdosing studies. Curr. Opin. Drug Discov. Devel. 2008; 11:104–110.
12. Bart J, et al. Quantitative assessment of P-glycoprotein function in the rat blood-brain barrier by distribution volume of [^{11}C]verapamil measured with PET. Neuroimage. 2003; 20:1775–1782. [PubMed: 14642487]
13. Sasongko L, et al. Imaging P-glycoprotein transport activity at the human blood-brain barrier with positron emission tomography. Clin. Pharmacol. Ther. 2005; 77:503–514. [PubMed: 15961982]
14. Lee YJ, et al. In vivo evaluation of P-glycoprotein function at the blood-brain barrier in nonhuman primates using [^{11}C]verapamil. J. Pharmacol. Exp. Ther. 2006; 316:647–653. [PubMed: 16293715]
15. Liow JS, et al. P-glycoprotein function at the blood-brain barrier imaged using ^{11}C-N-desmethyl-loperamide in monkeys. J. Nucl. Med. 2009; 50:108–115. [PubMed: 19091890]
16. Bankstahl JP, et al. Tariquidar-induced P-glycoprotein inhibition at the rat blood-brain barrier studied with (R)-^{11}C-verapamil and PET. J. Nucl. Med. 2008; 49:1328–1335. [PubMed: 18632828]
17. Wagner CC, et al. A pilot study to assess the efficacy of tariquidar to inhibit P-glycoprotein at the human blood-brain barrier with (R)–^{11}C-verapamil and PET. J. Nucl. Med. 2009; 50:1954–1961. [PubMed: 19910428]
18. Eyal S, et al. Regional P-glycoprotein activity and inhibition at the human blood-brain barrier as imaged by positron emission tomography. Clin. Pharmacol. Ther. 2010; 87:579–585. [PubMed: 20336065]
19. Kuntner C, et al. Dose-response assessment of tariquidar and elacridar and regional quantification of P-glycoprotein inhibition at the rat blood-brain barrier using (R)-[^{11}C]verapamil PET. Eur. J. Nucl. Med. Mol. Imaging. 2010; 37:942–953. [PubMed: 20016890]
20. Kreisl WC, et al. P-glycoprotein function at the blood-brain barrier in humans can be quantified with the substrate radiotracer ^{11}C-N-desmethyl-loperamide. J. Nucl. Med. 2010; 51:559–566. [PubMed: 20237038]
21. Passchier J, et al. Blood brain barrier permeability of [^{11}C]loperamide in humans under normal and impaired P-glycoprotein function [symposium abstract]. J. Nucl. Med. 2008; 49:211P.
22. Eyal S, Hsiao P, Unadkat JD. Drug interactions at the blood-brain barrier: fact or fantasy? Pharmacol. Ther. 2009; 123:80–104. [PubMed: 19393264]
23. Fox E, Bates SE. Tariquidar (XR9576): a P-glycoprotein drug efflux pump inhibitor. Expert Rev. Anticancer Ther. 2007; 7:447–459. [PubMed: 17428165]
24. Luurtsema G, Molthoff CF, Schuit RC, Windhorst AD, Lammertsma AA, Franssen EJ. Evaluation of (R)-[^{11}C]verapamil as PET tracer of P-glycoprotein function in the blood-brain barrier: kinetics and metabolism in the rat. Nucl. Med. Biol. 2005; 32:87–93. [PubMed: 15691665]
25. Toornvliet R, et al. Effect of age on functional P-glycoprotein in the blood-brain barrier measured by use of (R)-[^{11}C]verapamil and positron emission tomography. Clin. Pharmacol. Ther. 2006; 79:540–548. [PubMed: 16765142]
26. Lubberink M, et al. Evaluation of tracer kinetic models for quantification of P-glycoprotein function using (R)-[^{11}C]verapamil and PET. J. Cereb. Blood Flow Metab. 2007; 27:424–433. [PubMed: 16757979]
27. Stewart A, Steiner J, Mellows G, Laguda B, Norris D, Bevan P. Phase I trial of XR9576 in healthy volunteers demonstrates modulation of P-glycoprotein in CD56+ lymphocytes after oral and intravenous administration. Clin. Cancer Res. 2000; 6:4186–4191. [PubMed: 11106230]
28. Choo EF, et al. Differential in vivo sensitivity to inhibition of P-glycoprotein located in lymphocytes, testes, and the blood-brain barrier. J. Pharmacol. Exp. Ther. 2006; 317:1012–1018. [PubMed: 16537797]

29. Bankstahl JP, et al. A novel PET imaging protocol identifies seizure-induced regional overactivity of P-glycoprotein at the blood-brain barrier. J. Neurosci. 2011; 31:8803–8811. [PubMed: 21677164]
30. Kühnle M, et al. Potent and selective inhibitors of breast cancer resistance protein (ABCG2) derived from the p-glycoprotein (ABCB1) modulator tariquidar. J. Med. Chem. 2009; 52:1190–1197. [PubMed: 19170519]
31. Kuntner C, et al. Evaluation of [^{11}C]elacridar and [^{11}C]tariquidar in transporter knockout mice using small-animal PET [symposium abstract]. Neuroimage. 2010; 52:S25.
32. Muzi M, et al. Imaging of cyclosporine inhibition of P-glycoprotein activity using ^{11}C-verapamil in the brain: studies of healthy humans. J. Nucl. Med. 2009; 50:1267–1275. [PubMed: 19617341]
33. Mahar Doan KM, et al. Passive permeability and P-glycoprotein-mediated efflux differentiate central nervous system (CNS) and non-CNS marketed drugs. J. Pharmacol. Exp. Ther. 2002; 303:1029–1037. [PubMed: 12438524]
34. Hsiao, P.; Unadkat, JD. P-glycoprotein (P-gp)-based loperamide-cyclosporine A interaction at the blood-brain barrier, extrapolation from rat to human [symposium abstract]; AAPS Annual Meeting; New Orleans, USA. 2010;
35. Hsiao P, et al. Verapamil P-glycoprotein transport across the rat blood-brain barrier: cyclosporine, a concentration inhibition analysis, and comparison with human data. J. Pharmacol. Exp. Ther. 2006; 317:704–710. [PubMed: 16415090]
36. Lumen AA, Acharya P, Polli JW, Ayrton A, Ellens H, Bentz J. If the KI is defined by the free energy of binding to P-glycoprotein, which kinetic parameters define the IC50 for the Madin-Darby canine kidney II cell line overexpressing human multidrug resistance 1 confluent cell monolayer? Drug Metabol. Dispos. 2010; 38:260–269.
37. Zhou Q, Guo P, Kruh GD, Vicini P, Wang X, Gallo JM. Predicting human tumor drug concentrations from a preclinical pharmacokinetic model of temozolomide brain disposition. Clin. Cancer Res. 2007; 13:4271–4279. [PubMed: 17634557]
38. Investigator Brochure. Tariquidar (XR9576). P-Glycoprotein Pump Inhibitor. Aväant Pharmaceuticals Inc; Version Number: 11. Issue Date: 28 May 2007
39. Abrahim A, et al. Peripheral metabolism of (R)-[^{11}C]verapamil in epilepsy patients. Eur. J. Nucl. Med. Mol. Imaging. 2008; 35:116–123. [PubMed: 17846766]
40. Hammers A, et al. Three-dimensional maximum probability atlas of the human brain, with particular reference to the temporal lobe. Hum. Brain Mapp. 2003; 19:224–247. [PubMed: 12874777]
41. Langer O, et al. Pharmacoresistance in epilepsy: a pilot PET study with the P-glycoprotein substrate R-[^{11}C]verapamil. Epilepsia. 2007; 48:1774–1784. [PubMed: 17484754]

Europe PMC Funders Author Manuscripts

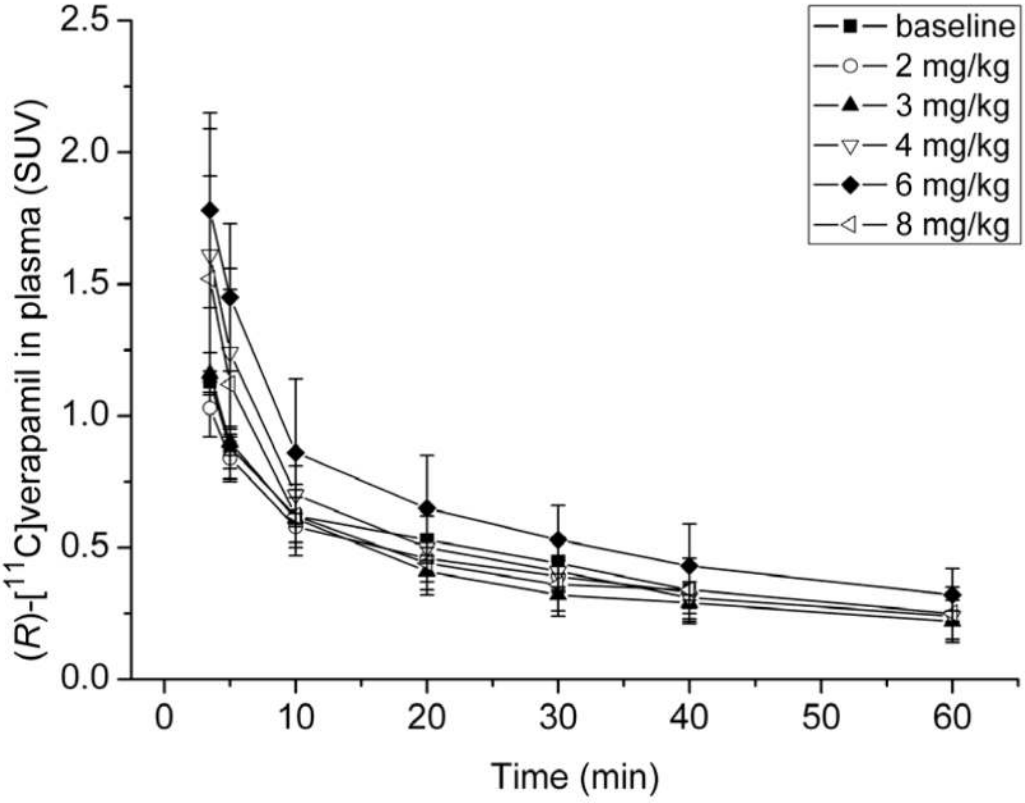

Figure 1.

Mean time-activity curves (standardized uptake value, SUV ±standard deviation, SD) of unmetabolized (*R*)-[^{11}C]verapamil in arterial plasma from 3.5 to 40 min after radiotracer injection for baseline scans (i.e. without tariquidar administration, *n*=5) and scans after administration of 2 mg/kg tariquidar (*n*=5) and from 3.5 to 60 min after radiotracer injection for scans after administration of 3, 4, 6 and 8 mg/kg tariquidar (*n*=3 per dose group).

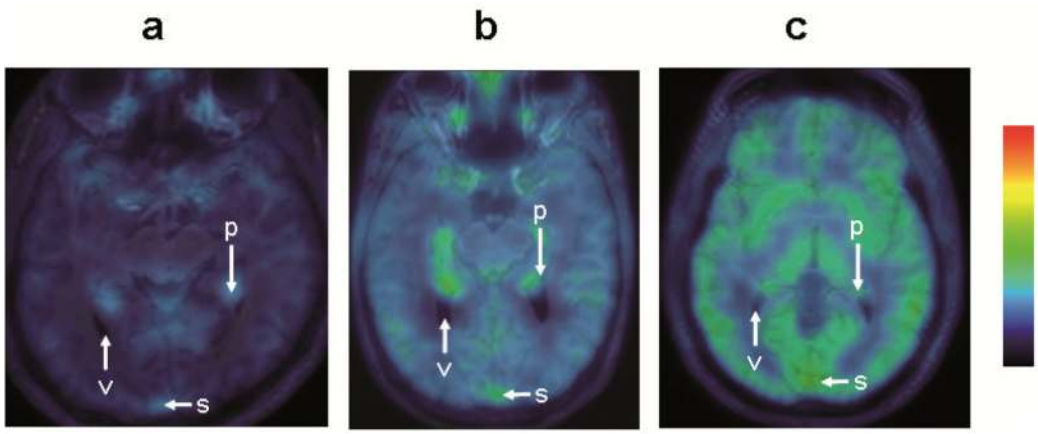

Figure 2.
Representative transaxial MRIs merged with (*R*)-[^{11}C]verapamil PET summation images (0-40 min) for a baseline scan (**a**, taken from reference (17)) and scans after administration of tariquidar at a dose of 3 mg/kg (**b**) and 8 mg/kg (**c**). Activity concentration is expressed as standardized uptake value (SUV) and radiation scale is set from 0.1 to 3.0. Anatomical structures are labeled using white arrows (v, ventricle; p, choroid plexus; s, venous sinus).

Europe PMC Funders Author Manuscripts

Europe PMC Funders Author Manuscripts

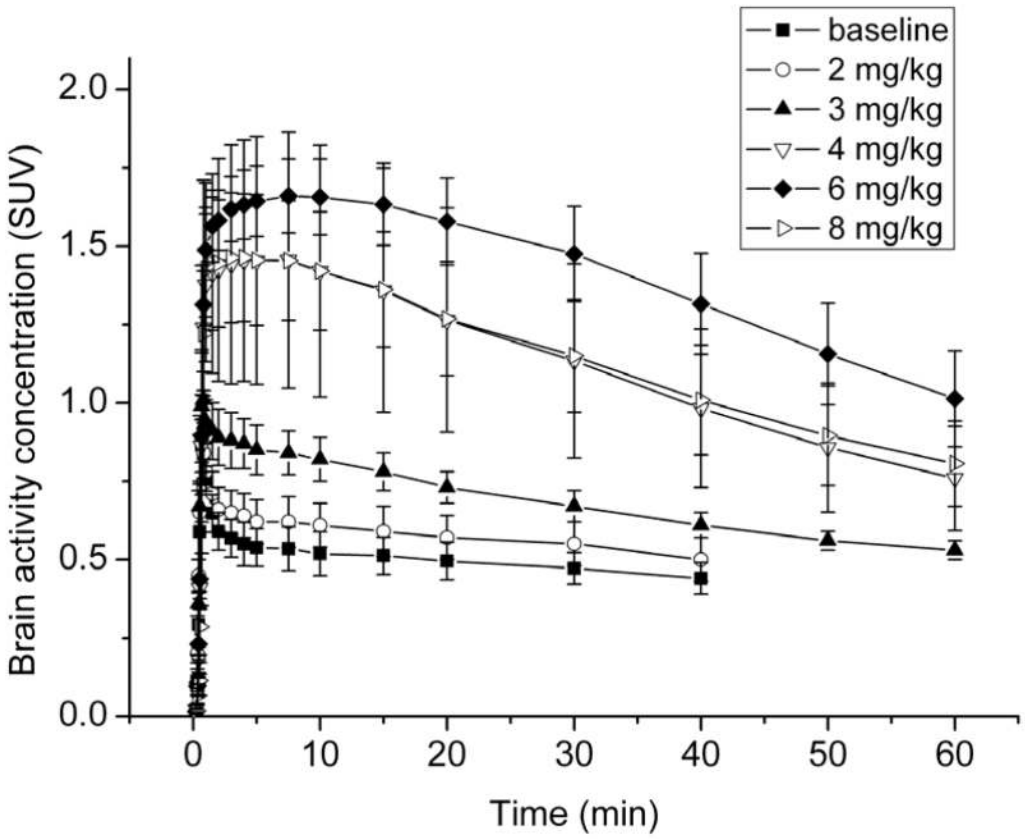

Figure 3.

Mean time-activity curves (standardized uptake value, SUV±SD) of (*R*)-[^{11}C]verapamil in whole brain grey matter from 0 to 40 min after radiotracer injection for baseline scans (i.e. without tariquidar administration, *n*=5) and scans after administration of 2 mg/kg tariquidar (*n*=5) and from 0 to 60 min after radiotracer injection for scans after administration of 3, 4, 6 and 8 mg/kg tariquidar (*n*=3 per dose group).

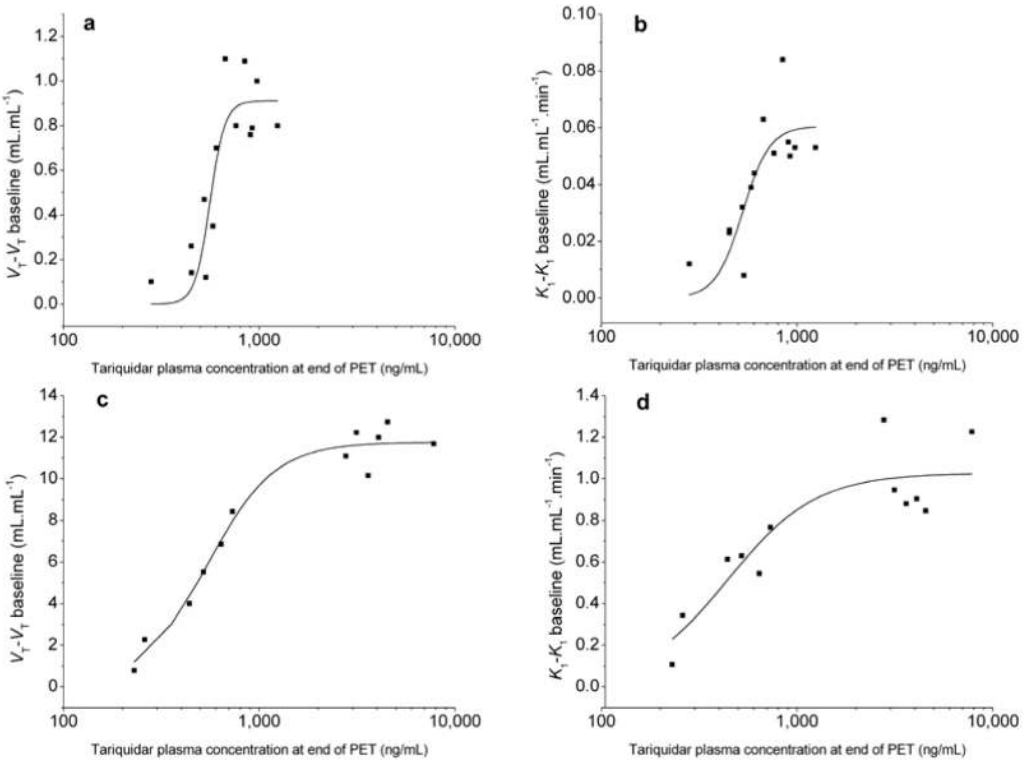

Figure 4.

Relationship between tariquidar plasma levels (ng/mL) at the end of the PET scan and (*R*)-[^{11}C]verapamil whole brain volume of distribution V_T- V_T at baseline and influx rate constant K_1-K_1 at baseline derived from 2-tissue-4-rate constant compartment model from 0-40 min in humans (**a**, **b**) and from 0-60 min in Sprague-Dawley rats (**c**,**d**) (19) and corresponding sigmoidal fits using the Hill function.

Europe PMC Funders Author Manuscripts

Europe PMC Funders Author Manuscripts

Table 1

Outcome parameters (whole brain) of 2-tissue-4-rate constant (2T4K)[a] and 1-tissue-2-rate constant (1T2K)[b] compartment model for baseline scans and scans after administration of different tariquidar doses

Tariquidar dose (mg/kg)[c]	K_1 (2T4K) (mL·mL^{-1}·min^{-1})	k_2 (2T4K) (min^{-1})	k_3 (2T4K) (min^{-1})	k_4 (2T4K) (min^{-1})	V_T (2T4K) (mL·mL^{-1})	K_1 (1T2K) (mL·mL^{-1}·min^{-1})
0	0.036±0.009 (13)	0.102±0.003 (83)	0.140±0.038 (158)	0.157±0.051 (53)	0.660±0.123 (5)	0.035±0.009 (6)
2	0.051±0.008 (11)	0.123±0.052 (57)	0.156±0.080 (123)	0.191±0.063 (42)	0.788±0.087 (2)	0.051±0.006 (6)
3	0.072±0.003 (7)	0.130±0.011 (45)	0.164±0.024 (100)	0.209±0.016 (32)	0.993±0.015 (2)	0.074±0.002 (5)
4	0.089±0.027 (4)	0.103±0.002 (31)	0.110±0.010 (94)	0.173±0.047 (31)	1.413±0.313 (1)	0.088±0.027 (3)
6	0.089±0.003 (5)	0.126±0.025 (26)	0.240±0.046 (49)	0.215±0.015 (27)	1.510±0.131 (1)	0.085±0.001 (3)
8	0.092±0.006 (13)	0.104±0.005 (58)	0.140±0.049 (112)	0.177±0.024 (27)	1.560±0.173 (2)	0.090±0.005 (4)

K_1, K_2, K_3, K_4, rate constants for transfer of activity between the plasma, the first and the second tissue compartments; V_T, volume of distribution.

Outcome parameters are given as mean ± standard deviation averaged over all subjects per dose group. The value in parentheses represents the precision of parameter estimates (expressed as their coefficient of variation in percent), averaged over all subjects per dose group.

[a] For 2T4K model data from 0-40 min after radiotracer injection were used.

[b] For 1T2K model data from 0-10 min after radiotracer injection were used.

[c] For 0 and 2 mg/kg: n=5 (data taken from (17)); for the other dose groups: n=3 per dose.

Table 2

Parameter estimates for sigmoidal curve fits of tariquidar concentration[a] *versus* effect measures in humans and rats

Effect measure (human)[b]	E_{max}	EC_{50} (ng/mL)	*n*	R^2
V_T–V_T baseline (2T4K)[c]	0.9±0.1	561±24	11.3±5.4	0.789
K_1–K_1 baseline (2T4K)[c]	0.061 ±0.008	526±41	6.3±3.5	0.668
K_1–K_1 baseline (1T2K)[d]	0.059±0.007	521±40	6.2±3.5	0.673
Effect measure (rat) [e]	E_{max}	EC_{50} (ng/mL)	*n*	R^2
V_T–V_T baseline[c] (2T4K)[f]	11.8±0.3	544±32	2.5±0.5	0.974
K_1–K_1 baseline[c] (2T4K)[f]	1.0±0.1	441±81	1.9±0.8	0.812

E_{max}, maximum effect; EC_{50}, half-maximum effect concentration of tariquidar in plasma (ng/mL); *n*, Hill coefficient; R^2, coefficient of determination; V_T, volume of distribution; K_1, influx rate constant from plasma into first brain tissue compartment; 2T4K, 2-tissue-4-rate constant compartment model; 1T2K, 1-tissue-2-rate constant compartment model.

[a] Tariquidar plasma concentrations at end of PET scan measured with liquid chromatography tandem mass spectrometry.

[b] Baseline values in humans: V_T (2T4K), 0.66±0.12; K_1 (2T4K), 0.036±0.01; K_1 (1T2K), 0.035±0.01.

[c] Data from 0-40 min after radiotracer injection were used.

[d] Data from 0-10 min after radiotracer injection were used.

[e] Baseline values in rats: V_T (2T4K), 1.27±0.15; K_1 (2T4K), 0.16±0.05.

[f] Data from 0-60 min after radiotracer injection were used.